Thin-Walled Structures **2** (1984) 165–174

Particular Points of Elastic Analysis of Clad Pitched Roof Portal Frame Structures

J. M. Franssen

Department 'Ponts et Charpentes', University of Liege, 6, Quai Banning, Liege, Belgium

ABSTRACT

This paper deals with the elastic analysis of clad pitched roof portal frame structures.

A practical structure is analysed, first neglecting the stiffening effect of sheeting and then according to the rules of stressed skin design. The differences between both analyses are shown.

Different aspects of stressed skin design analysis are investigated, namely:

1. *The fact that some vertical loads mobilize the diaphragm effect, whereas others do not.*
2. *The modification of axial forces in the columns, due to the influence of diaphragm action.*
3. *The assumption that shear forces are transmitted from sheeting to the eaves of the frames.*

1 INTRODUCTION

It is now well known that realistic analysis of clad structures cannot be carried out unless the diaphragm effect is taken into account. The principles of such an analysis have been laid down[1,2] and European Recommendations about the determination of diaphragm characteristics have been published.[3]

The author's purpose is to investigate the following points of the elastic

Thin-Walled Structures 0263-8231/84/$03·00

analysis of clad pitched roof portal frame structures to which, in his view, not enough attention has been paid:

1. The ability of dead loads to mobilize the diaphragm effect.
2. The influence of diaphragm action on axial forces in the columns.
3. The transmission of shear forces from sheeting to the frames.

In order to be as clear as possible, limited consideration has been given to symmetrical vertical loads, but most of the conclusions drawn could be generalized to any case of loading.

Throughout this paper, a practical example has been developed in order to provide some support to the discussion and to draw interesting numerical values.

2 BARE FRAMES

Before the principles of diaphragm action were laid down the stiffening effect of sheeting was not taken into account when calculating a structure (and this is still frequently the case). If the stiffening effect is not taken into account, every frame can be analysed separately and only the structural member carries loads.

Such an analysis has been carried out, partly for comparative purposes and partly because some of the results will be utilized later in the analysis of the clad structure. The design example is shown in Fig. 1.

2.1 Frame specifications

Frames of uniform section with pinned bases
Type: 457 × 191 × 67 kg/m. U.B.
Area: 85·4 cm^2.
Second moment of area: $I = 29\ 337\ cm^4$.
Cladding panels
Flexibility: $c = 0{\cdot}10$ mm/kN.
Vertical line loads
Characteristic dead load: $p_k = 4$ kN/m, $\gamma = 1{\cdot}33$.
Characteristic imposed load: $p_k = 7$ kN/m, $\gamma = 1{\cdot}5$.
Total characteristic load: $p_k = 11$ kN/m.
Basic design load: $p^* = 0{\cdot}9 \times 1{\cdot}33 \times 4 + 1{\cdot}5 \times 7 = 15{\cdot}29$ kN/m.

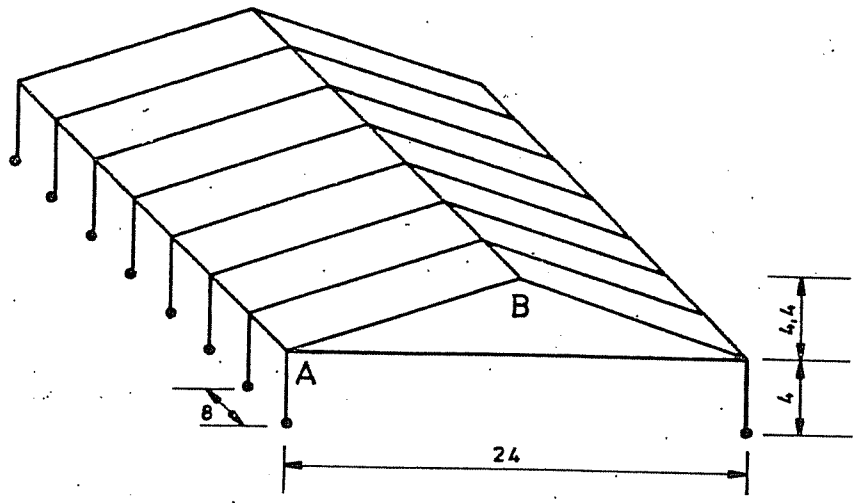

Fig. 1. Design example.

2.2 Results for bare frames

Results of a manual analysis (neglecting the effect of axial strains) can be found in Appendix 1, Table A1.1. From this it is noted that

1. Maximum bending moment: $M_A^* = -475$ kN/m.
2. Eaves deflections: $u_k = 31{\cdot}3$ mm.
3. Rafter deflection: $f_k = 84{\cdot}3$ mm.

3 USUAL STRESSED SKIN DESIGN

The usual way to take the cladding into account is to replace the shear panels by horizontal 'springs' supporting each frame i at its eaves by a force

$$R_i = (1-\eta_i)S$$

where S = restraining forces, and η_i = reduction factor for frame i (depending on the relative flexibility of the structure) (Fig. 2).

Due to the inclination of the roof, the diaphragm carries a load

$$P_i = R_i/\cos\theta = (1-\eta_i)(S/\cos\theta)$$

to provide a support R_i to the frames. Thus we get:

Spread flexibility: $k_{sp} = 0{\cdot}185$ mm/kN.
Restraining forces: $S = 235{\cdot}6$ kN.
Relative flexibility: $\psi_{sp} = 0{\cdot}614$.
Reduction factors: $\eta_2 = \eta_7 = 0{\cdot}526$
$\eta_3 = \eta_6 = 0{\cdot}762$
$\eta_4 = \eta_5 = 0{\cdot}853$

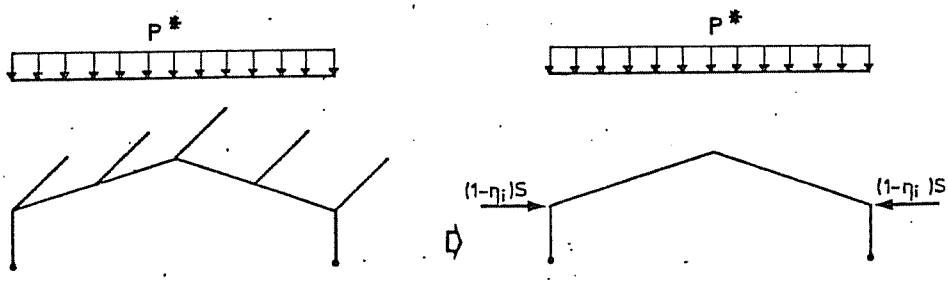

Fig. 2. Usual stressed skin design.

Calculated deflections and bending moments are given in Appendix 1, Table A1.2. The maximum values are:

Bending moment: $M_A^* = -424$ kNm (-11%).
Eaves deflections: $u_k = 26{\cdot}7$ mm (-15%).
Rafter deflection: $f_k = 71{\cdot}0$ mm (-16%).
Shear in diaphragm: $V^* = 216$ kN.

Comparison between the values from Sections 2 and 3, as well as the important shear force induced in the diaphragm, show that it is necessary to consider the effect of the cladding on the distribution of vertical loads.

4 DISTRIBUTION OF DEAD LOADS

In this section the distribution of dead loads through the frames and cladding will be investigated.

It is apparent that the diaphragm effect will only be effective under loads applied after the sheeting has been fastened to the frames. Thus:

1. The skin effect cannot help in carrying the dead load of the rafters since the sheeting is not present when this load is applied.
2. The same reasoning can be applied to the purlins.
3. In the same way, the weight of the sheeting will only cause bending in the frames, as the sheets must first be placed on the purlins before they are fastened.
4. Nevertheless, the diaphragm effect is quite effective under the dead load of the insulation and watertight membrane.

Thus a stressed skin structure can be compared to a composite concrete structure, the dead load of which is supported by steel beams. Concrete can only carry loads when it has set.

The design example is carried out using the following data:

Dead load of rafters: $p_k = 0{\cdot}67$ kN/m.
Five purlins on each slope: $A = 5$ cm^2 (Ref. 2).
$p_k = 0{\cdot}13$ kN/m.
Sheeting: $0{\cdot}1$ kN/m^2 $p_k = 0{\cdot}80$ kN/m.

Therefore for loads with no diaphragm effect: $p_k = 1{\cdot}60$ kN/m, and $p^* = 1{\cdot}915$ kN/m; and for loads producing a diaphragm effect: $p_k = 9{\cdot}40$ kN/m, and $p^* = 13{\cdot}375$ kN/m.

The analysis is carried out in a similar manner to that in Section 3 except that the restraining forces S now refer just to those loads which produce a diaphragm effect.

From Table A1.3 of Appendix 1, we get

$M_A^* = -431$ kN/m $(+1{\cdot}5\%)$.
$u_k = 27{\cdot}4$ mm $(+2{\cdot}5\%)$.
$f_k = 73{\cdot}0$ mm $(+2{\cdot}7\%)$.
$V^* = 189$ kN $(-12{\cdot}5\%)$.

If the above results are compared to the usual stressed skin analysis, we notice that the differences are small regarding bending moments and deflections of the frames, but that a more significant decrease occurs in the shear forces in the cladding panels. This decrease is affected by:

1. The importance of loads with no diaphragm effect compared with total loads.
2. The importance of the skin effect in the structure, e.g. a steep roof pitch and a short building length[4] will increase the stressed skin effect.

5 AXIAL FORCES IN COLUMNS

In this section only those loads which produce a diaphragm effect are considered (see Section 4).

The usual stressed skin analysis determines, for each frame i, the horizontal supporting force due to the sheeting $R_i = (1 - \eta_i)S$ (see Fig. 2). The inclination θ of the roof is taken into account when considering that the diaphragm carries a load $P_i = R_i/\cos\theta$ to provide a support R_i to the frame i.

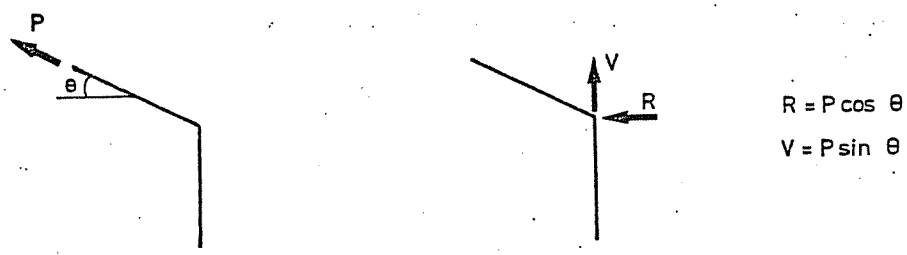

Fig. 3. Resolution of the supporting force.

A more complete consideration (Fig. 3) shows that the vertical component of the supporting force reduces the axial force in column due to vertical loads.

The analysis gives the value of $R_i = (1 - \eta_i)S$, hence

$$P_i = R_i/\cos\theta = (1-\eta_i)S/\cos\theta$$

and

$$V_i = P_i \sin\theta = R_i \tan\theta = (1-\eta_i)S\tan\theta$$

The vertical force V_i reduces the compression in the columns of the frames and must be taken into account. In the same way, due to the inclination of the roof, the end gables are submitted to a vertical force equal and opposite to the forces V from the intermediate frames and applied to the apex of the gables (Fig. 4).

In the design example, the compression in the columns of the intermediate frames (183·5 kN by the usual analysis) moderates to the following values when the effect of forces V has been taken into account

Frames 2 and 7: N^* = 147·kN (−20%).
Frames 3 and 6: N^* = 166 kN (−10%).
Frames 4 and 5: N^* = 172 kN (−6%).

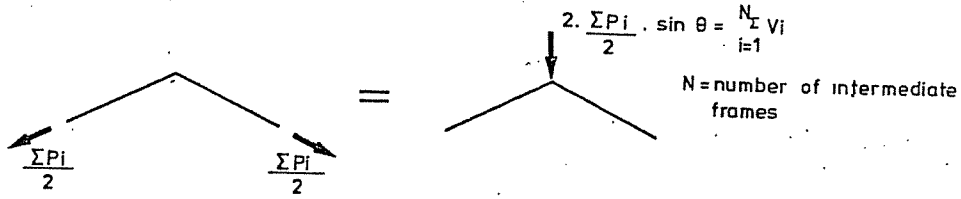

Fig. 4. End gables.

The minimum decrease observed (the columns are designed for the maximum load) is not very important. However, the value of the point load transmitted to each end gable is 132 kN, which is not negligible compared with 183·5 kN of distributed load and so it must be considered under bending and stability conditions.

In the same way as in Section 4, it can be shown that the effect of diaphragm action on axial forces in the columns is even more important when the length of the structure is short and the roof slope is high.

6 TRANSMISSION OF SHEAR FORCES FROM SHEETING TO FRAMES

When analysing the structure in the preceding sections it has been assumed that the forces transmitted from the diaphragms to the frames consist of point loads applied to the eaves (Fig. 3). However, transmission of shear forces takes place along the whole length of the rafter through sheet to rafter fasteners (decking parallel to span) or through sheet to shear connector fasteners and purlin to rafter connections (decking perpendicular to span). In order to estimate the influence of this assumption, an analysis of the central frame of the previous design example has been carried out: (1) to the distributed vertical load; and (2) to the supporting force from the diaphragm that was first considered as a point load at the eaves, and that then was considered as uniformly distributed on the rafters.

Appendix 2 presents the important results from both analyses as illustrated in Fig. 5. Concerning the point load, the slight differences between the computer output and results of the manual analysis are due to the influence of axial strains that are significant in the computer analysis and ignored in the manual analysis.

As expected, the modification of point load into distributed load has a

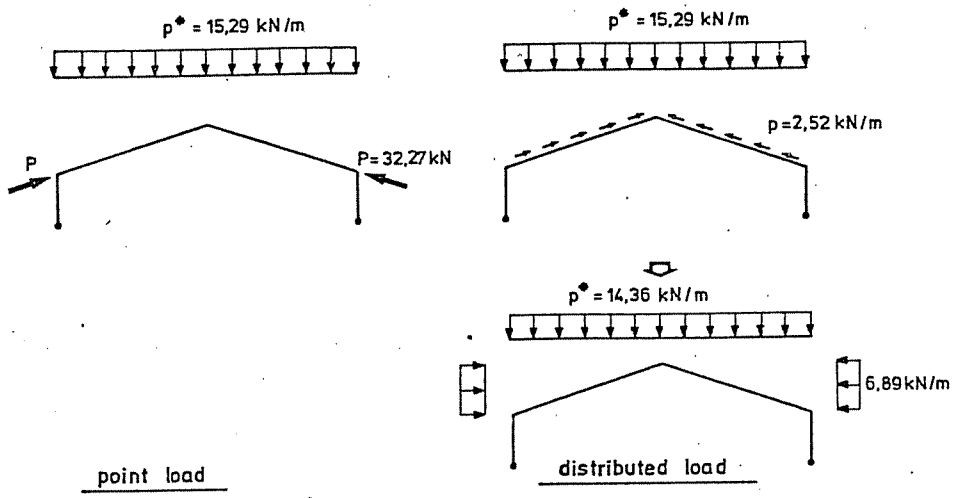

Fig. 5. Central frame—computer analysis.

significant influence only on the axial forces in the rafter. The reduction is 17%. If the decrease of axial force is important for stability conditions, it must be noted that the maximum axial stress in the rafter, σ_{max}^{rafter} (due to bending moment and to axial force) is not significantly modified.

It can be concluded from this that the hypothesis of taking a point load for the shear force from the diaphragm to the frame is justified regarding the analysis of intermediate frames.

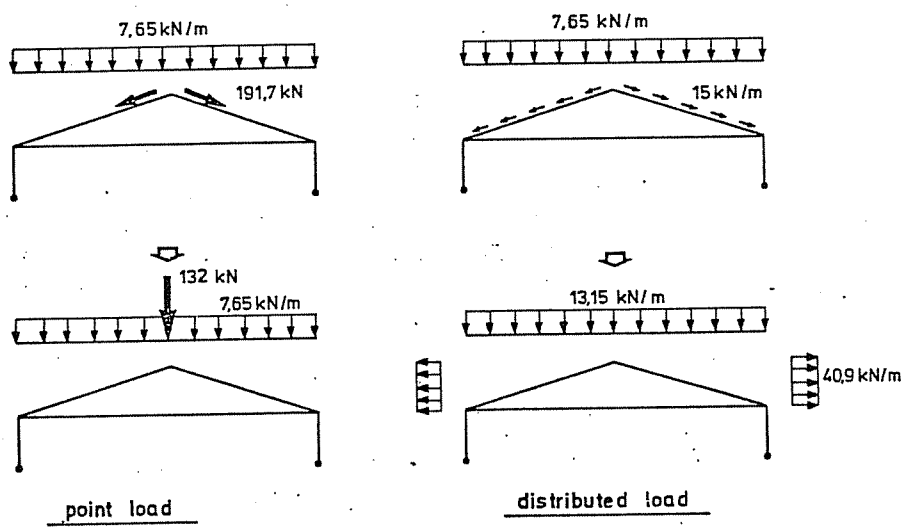

Fig. 6. End gable.

However, due to the importance of shear forces transmitted to the rafter, it is advisable to take this effect into account when analysing end gables (Fig. 6).

7 CONCLUSIONS

In this paper, it has been shown that it may be important to distinguish which part of the dead load has nothing to do with diaphragm action. The interest of this more precise analysis lies in the fact that it leads to a lower value of maximum shear forces in cladding panels.

It is shown how the diaphragm action of the sheeting reduces axial forces in the columns of the intermediate frames and why this effect could be important in the design of end gables.

It is also shown that it is permissible to assume that supporting forces from diaphragms to frames are point forces when analysing intermediate frames, but that more attention should be paid to end gables.

REFERENCES

1. Bryan, E. R., *The stressed skin design of steel buildings*, London, Crosby Lockwood, 1973.
2. Davies, J. M. and Bryan, E. R., *Manual of stressed skin diaphragm design*, London, Granada Publishing, 1982.
3. ECCS-XVIII-77-IE, *European recommendations for the stressed skin design of steel structures*, 1976.
4. Franssen, J. M., Evaluation quantitative et qualitative de la collaboration des toitures en tôles minces, *Construction Métallique, C.T.I.C.M.*, **2** (1983) 65–75.

APPENDIX 1—MANUAL ANALYSIS

TABLE A1.1
Bare Frame

M^*_A	−475 kNm
M^*_B	104 kNm
u_k	31·3 mm
f_k	84·3 mm
V^*	0

TABLE A1.2
Usual Stressed Skin Design[a]

	Frame 2 (7)	*Frame 3 (6)*	*Frame 4 (5)*
η_i	0·526	0·762	0·853
M^*_A (kNm)	−312	−393	−424
M^*_B (kNm)	−44·7	29·1	57·6
u_k (mm)	16·5	23·9	26·7
f_k (mm)	44·5	64·3	71·0
V^* (kN)	216	96·6	36·9

[a]Maximum values are underlined.

TABLE A1.3
Distribution of Dead Load[a]

	Frame 2 (7)	*Frame 3 (6)*	*Frame 4 (5)*
M^*_A (kNm)	−332	−403	−431
M^*_B (kNm)	−26·1	38·4	63·4
u_k (mm)	18·6	25·0	27·4
f_k (mm)	50·3	67·2	73·0
V^* (kN)	189	84·5	32·3

[a]Maximum values are underlined.

APPENDIX 2—COMPUTER ANALYSIS

TABLE A2.1
Value for Frame 4 (5)

	Point force	*Distributed force*
M^*_A (kNm)	−428	−430
M^*_B (kNm)	48·4	48·2
u_k (mm)	25·1	25·2
f_k (mm)	72·6	72·7
V^* (kN)	32·3	32·3
$N^{*\,\text{column}}$ (kN)	174	174
$N^{*\,\text{rafter}}_{\text{max}}$ (kN)	195	163
$\sigma^{\text{rafter}}_{\text{max}}$ (kN/cm^2)	35·6	35·4